eNeuro Accepted Manuscript

eNeuro

Research Article: Confirmation | Integrative Systems

Arousal-state dependent alterations in VTA-GABAergic neuronal activity

https://doi.org/10.1523/ENEURO.0356-19.2020

Cite as: eNeuro 2020; 10.1523/ENEURO.0356-19.2020

Received: 28 August 2019
Revised: 8 January 2020
Accepted: 29 January 2020

This Early Release article has been peer-reviewed and accepted, but has not been through the composition and copyediting processes. The final version may differ slightly in style or formatting and will contain links to any extended data.

Alerts: Sign up at www.eneuro.org/alerts to receive customized email alerts when the fully formatted version of this article is published.

Copyright © 2020 Eban-Rothschild et al.
This is an open-access article distributed under the terms of the Creative Commons Attribution 4.0 International license, which permits unrestricted use, distribution and reproduction in any medium provided that the original work is properly attributed.

eNeuro Accepted Manuscript

1. **Manuscript Title:** Arousal-state dependent alterations in VTA-GABAergic neuronal activity

2. **Abbreviated Title**: VTA-GABA and arousal

3. **List of authors:**

Ada Eban-Rothschild[1,2]
Jeremy C. Borniger[2]
Gideon Rothschild[1]
William J. Giardino[2]
Joshua G. Morrow[1]
Luis de Lecea[2]

[1]Department of Psychology, University of Michigan 4067 East Hall, 530 Church St. Ann Arbor, MI 48109
[2]Department of Psychiatry & Behavioral Sciences, Stanford University, P154 MSLS Building, 1201 Welch Rd, Stanford, CA 94305

4. **Author Contributions:**
AER and LdL designed research; AER, JCB, WJG and JGM performed research, GR contributed analytic tools. AER analyzed data. AER, JCB and LdL Wrote the paper.

5. **Correspondence should be addressed to**

Ada Eban-Rothschild
Department of Psychology
University of Michigan
4067 East Hall, 530 Church St.
Ann Arbor, MI 48109
adae@umich.edu

Luis de Lecea
Department of Psychiatry & Behavioral Sciences
Stanford University
P154 MSLS Building, 1201 Welch Rd
Stanford, CA 94305
llecea@stanford.edu

6. **Number of Figures = 5**
7. **Number of Tables = 0**
8. **Number of Multimedia = 0**
9. **Number of words for Abstract = 248**
10. **Number of words for Significance Statement = 113**
11. **Number of words for Introduction = 526**
12. **Number of words for Discussion = 1834**
13. **Acknowledgements:**

We acknowledge the Stanford University laboratory animal facility personnel for providing excellent care to the animals used in these studies.

14. **Conflict of Interest:** Authors report no conflict of interest.

eNeuro Accepted Manuscript

15. Funding sources:
A.E-R. is supported by Alfred P. Sloan Foundation, the Frances & Kenneth Eisenberg Translational Research Award, the NARSAD Young Investigator Grant # 27297, Kavli Innovators Research Award, and the National Institutes of Health 1RF1MH120005-01., J.C.B. is supported by an NIH F32MH115431, W.J.G. is supported by K99 AA025677, and L.d.L is supported by the National Institutes of Health grants R01 MH087592 and R01 MH102638. We also recognize support from A. Olson and the Stanford Neuroscience Microscopy Service, NIH NS069375.

Abstract

Decades of research have implicated the ventral tegmental area (VTA) in motivation, learning and reward processing. We and others recently demonstrated that it also serves as an important node in sleep/wake regulation. Specifically, VTA-dopaminergic neuron activation is sufficient to drive wakefulness and necessary for the maintenance of wakefulness. However, the role of VTA-GABAergic neurons in arousal regulation is not fully understood. It is still unclear whether VTA-GABAergic neurons predictably alter their activity across arousal states, what is the nature of interactions between VTA-GABAergic activity and cortical oscillations, and how activity in VTA-GABAergic neurons relates to VTA-dopaminergic neurons in the context of sleep/wake regulation. To address these, we simultaneously recorded population activity from VTA-subpopulations and EEG/EMG signals during spontaneous sleep/wake states and in the presence of salient stimuli in freely-behaving mice. We found that VTA-GABAergic neurons exhibit robust arousal-state-dependent alterations in population activity, with high activity and transients during wakefulness and REM sleep. During wakefulness, population activity of VTA-GABAergic neurons, but not VTA-dopaminergic neurons, was

eNeuro Accepted Manuscript

positively correlated with EEG gamma power and negatively correlated with theta power. During NREM sleep, population activity in both VTA-GABAergic and VTA-dopaminergic neurons negatively correlated with delta, theta, and sigma power bands. Salient stimuli, with both positive and negative valence, activated VTA-GABAergic neurons. Together, our data indicate that VTA-GABAergic neurons, like their dopaminergic counterparts, drastically alter their activity across sleep-wake states. Changes in their activity predicts cortical oscillatory patterns reflected in the EEG, which are distinct from EEG spectra associated with dopaminergic neural activity.

Keywords: Arousal, GABA, dopamine, VTA, Fiber-photometry

Statement of Significance

Little is known about how ventral tegmental area (VTA) neural ensembles couple arousal to motivated behaviors. Using cell-type specific genetic tools, we investigated the population activity of GABAergic and dopaminergic neurons within the VTA across sleep/wake states and in the presence of salient stimuli. We demonstrate that

eNeuro Accepted Manuscript

coordinated neural activity within VTA-GABAergic neurons peaks during wakefulness and REM sleep. Furthermore, neuronal activity in VTA-GABAergic neurons is correlated with high frequency, low amplitude cortical oscillations during waking, but negatively correlated with high amplitude slower frequency oscillations during NREM sleep. Our results demonstrate that VTA-GABAergic neuronal activity is tightly linked to cortical arousal and highlight this population as a potential important node in sleep/wake regulation.

Introduction

Motivated behaviors are fundamentally linked to arousal, however, little is known about the neural mechanisms that couple motivational processes with sleep-wake regulation (Eban-Rothschild et al., 2018). The ventral tegmental area (VTA), which is comprised of 55-65% dopaminergic, 35-40% gamma-aminobutyric acid (GABA) and ~2% glutamatergic neurons (Nair-Roberts et al., 2008; Morales and Margolis, 2017), is a key brain structure in the regulation of motivation, reinforcement learning and reward processing (Berridge, 2007; Salamone and Correa, 2012; Berke, 2018). VTA-GABAergic neurons have been suggested to tightly control activity in intermingled VTA-dopaminergic neurons in the context of motivation and reward (Cohen et al., 2012; van Zessen et al., 2012), yet their regulatory role in the context of sleep and wakefulness is not fully understood.

Neuronal activity in the VTA exhibits arousal-state-dependent alterations, with increased activity during wakefulness and REM sleep compared to NREM sleep (Miller et al., 1983; Fifel et al., 2018). Although initial studies suggested that VTA-dopaminergic

eNeuro Accepted Manuscript

neurons do not change their mean firing rate across sleep/wake states (Miller et al., 1983; Steinfels et al., 1983), more recent examinations revealed marked arousal state-dependent alterations in both firing rate and firing pattern (Dahan et al., 2007; Gomperts et al., 2015). Moreover, using cell-type specific fiber photometry recordings, we demonstrated that at the population level, VTA-dopaminergic neurons show strong arousal-state-dependent alterations in activity (Eban-Rothschild et al., 2016). Early single-unit electrophysiology recordings in rats suggested that activity in VTA-GABAergic neurons varies significantly across arousal state, with high firing rates during active waking and REM sleep (Lee et al., 2001). An additional study demonstrated activation, via cFos immunolabeling, of VTA-GABAergic neurons following recovery from REM sleep deprivation (Maloney et al., 2002)–suggesting that these neurons influence or monitor discrete arousal states. Nonetheless, there is a great challenge to accurately differentiate between different cell types in freely moving wild type animals and conventional electrophysiological characteristics used to differentiate between VTA cell types has been debated (Margolis et al., 2006; Lammel et al., 2008; Ungless and Grace, 2012). Moreover, it is still unclear whether activity in VTA-GABAergic neurons precedes or lags behind arousal state transitions, how population activity in the VTA is related to different components of the cortical EEG and how VTA-GABAergic population dynamics relate to that of co-mingled dopaminergic neurons. A few recent studies have shed some light onto these questions, demonstrating that VTA-GABAergic neurons bidirectionally regulate wakefulness in part via their projections to the lateral hypothalamus (LH) (Takata et al., 2018; Chowdhury et al., 2019; Yu et al., 2019b). However, there are some critical discrepancies between these studies, as one suggests

eNeuro Accepted Manuscript

that VTA-GABAergic neurons are predominantly wake and REM sleep active (Yu et al., 2019), while the other provides evidence that these neurons fire mostly during NREM sleep (Chowdhury et al., 2019). Therefore, the exact phenotype of VTA-GABAergic neurons across arousal states remains unclear.

To address these questions, we used Cre-dependent viral vectors to express the calcium indicator GCaMP6 exclusively in either VTA-GABAergic or VTA-dopaminergic neurons. We then used fiber photometry in tandem with electroencephalography/electromyography (EEG/EMG) recordings to monitor spontaneous arousal-state dependent changes in population activity. We also recorded calcium and EEG measures during a battery of behavioral challenges (social and non-social).

Methods

Animals

We used adult (>8 wks old) male vesicular GABA transporter (Vgat)-ires-Cre (Jackson Labs stock #028862) knock-in mice backcrossed on the C57BL/6J wild-type background (for more than 10 generations) and tyrosine hydroxylase (Th)-IRES-Cre mice obtained from the European Mouse Mutant Archive and backcrossed on the C57BL/6J wild-type background (for more than 15 generations). During experiments, mice were individually housed in custom Plexiglas recording chambers at a constant temperature (23 ± 1°C), humidity (40-60%), and 12/12 light/dark cycle. Food (Laboratory Rodent Diet #5001) and water were available *ad libitum*. All experiments

eNeuro Accepted Manuscript

were performed in accordance with the guidelines described in the US National institutes of Health Guide for the Care and Use of Laboratory Animals and were approved by Stanford University's Administrative Panel on Laboratory Animal Care.

Virus preparation

Cre-dependent recombinant AAV vectors (pAAV-Ef1α-DIO-GCaMP6s, pAAV-Ef1α-DIO-GFP, and pAAV-Ef1α-DIO-GCaMP6f) were serotyped with AAV-DJ coat proteins and packaged by the Gene Vector and Virus Core at Stanford University. The final viral concentration was 1-1.5 x 10^{13} genome copies (gc) ml^{-1}. Aliquots of virus were stored at -80°C until stereotaxic injection.

Surgery

At the start of surgical procedures, mice were anesthetized with ketamine and xylazine (100 and 20 mg kg^{-1}, respectively; IP) and placed into a stereotaxic frame (David Kopf Instruments, Tujunga, CA, USA). To selectively target VTA-GABAergic neurons, virus was infused into the VTA (AP -3.3 mm; ML = 0.2 mm; DV = -4.6 mm) using a 33-guage internal cannula (Plastics One, Inc., Roanoke, VA) attached to a 10 µl Hamilton syringe, at a rate of 0.1 µl min^{-1} (400 nl total virus). After infusion, the internal cannula was kept in place for at least 8 min and then slowly withdrawn. Following virus injections, a 400 µm diameter monofiberoptic cannula (Doric lenses, Inc. Quebec, Canada) was lowered into the VTA (AP = -3.3, ML = 0.3; DV -4.3 mm) for fiber photometry recordings. Mice were also fitted with two gold-plated miniature screw electrodes (AP = 1.5 mm, ML = -1.5 mm and AP = -3.5 mm, ML = -2.8 mm) and two EMG wire electrodes (316SS/44T,

eNeuro Accepted Manuscript

Medwire), previously soldered to a four-pin connector (custom). These electrodes were inserted between the trapezius muscles for EMG measurements. The implant was secured to the skull with C&B Metabond (Parkell) and dental cement. The skin was closed with surgical sutures, and mice were maintained on a heating pad until fully mobile. Mice were allowed to recover from surgery for three weeks, and then acclimated to a flexible EEG/EMG connection cable and optical patch cord for ~10 d within individual recording chambers. Mice were continuously connected to the patch cord and EEG/EMG connection cable throughout the experiments.

Fiber photometry recordings and data analysis

Fiber photometry recordings were conducted as previously described (Lerner et al., 2015; Eban-Rothschild et al., 2016). We sinusoidally modulated blue light (30-50 µW) from a 470-nm excitation LED (M470F3, Thorlabs, NJ, USA) at 211 Hz, using a custom Matlab script (MathWorks, Natick, MA, USA) and a multifunction data acquisition device (NI USB-6259, National Instruments, Austin, TX, USA). The blue light was passed through a GFP excitation filter (MD498, Thorlabs), reflected off a dichroic mirror (MD498, Thorlabs), and coupled using a fiber collimation package (F240FC-A, Thorlabs) into a low-fluorescence patch cord (400 µm, 0.48 NA; Doric Lenses) connected to the implanted optic fiber (400 µm) by a zirconia sleeve. GCaMP6 signal was collected through the excitation patch cord, passed through a GFP emission filter (MF525-39, Thorlabs), and focused onto a photodetector (Model 2151, Newport, Irvine, CA, USA) using a lens (LA1540-A, Thorlabs). The signal was then sent to a lock-in amplifier (30-ms time constant, Model SR830, Stanford Research Systems, Sunnyvale,

eNeuro Accepted Manuscript

CA, USA) that was synchronized to 211 Hz. Signals from the amplifiers were collected at 1 kHz using a custom Matlab script and a multifunction data acquisition device (National Instruments).

The photometry signal was down-sampled using interpolation to match the EEG sampling rate of 256 Hz. For each experiment, the photometry signal F was converted to ΔF/F by $\Delta F/F(t) = \frac{F(t)-\text{median}(F)}{\text{median}(F)}$. To address a short decay at the beginning of some recording sessions, the $\Delta F/F$ signal from each session was fitted with a decreasing exponential of the form $a \times e^{bx}$, where $a > 0$ and $b < 0$. We then subtracted the exponential fit from the original $\Delta F/F$ signal. To detect calcium transients, we generated two filtered $\Delta F/F$ signals, one low-pass filtered at 0-0.4 Hz, and the other low-pass filtered at 0-40 Hz. We calculated a trace of the derivative of their squared difference and identified candidate transient times by thresholding this signal at mean +1.5 standard deviations. We further required that the $\Delta F/F$ of candidate transient times be higher than the mean +1.5 standard deviations of the trace. The exact peak time of each transient was identified by taking the maximal value of the thresholded signal within each transient. For each session and for each arousal state, we calculated the mean transient rate (calculated as the number of transients per second) and mean transient amplitude (calculated as the mean $\Delta F/F$ *at transient peak times).*

For sleep-wake analyses of Vgat-cre mice, we recorded data during 7-8 sessions per mouse (n=5), each 30-40 minute long, during the light phase. For sleep-wake analyses of Th-cre mice, we recorded data during 8 sessions per mouse (n=4), each 10-45-min long during the light phase. We used only sessions during which mice showed all three

eNeuro Accepted Manuscript

arousal states (wake, NREM, and REM sleep). For each session we calculated the mean $\Delta F/F$ during all times of wake, NREM sleep, and REM sleep. For state transition analyses, we identified all points of state transition and aligned $\Delta F/F$ around these times. Mean $\Delta F/F$ and transient rate of the Th-Cre mice analyzed in this paper were previously reported in Eban-Rothschild et al. 2016.

EEG/EMG recording and analysis

EEG/EMG signals were amplified (Grass Technologies) and digitized at 256 Hz using Vital Recorder software (Kissei Comtec America). Using analysis software (SleepSign for Animal, Kissei Comtec America) we filtered the signal (EEG: 0.3-80 Hz, EMG: 25-50 Hz) and spectrally analyzed it by fast Fourier transformation to determine a single arousal state (wake, NREM sleep or REM sleep) for each 4-s epoch of data. Wakefulness was defined as desynchronized low-amplitude EEG and heightened tonic EMG activity with phasic bursts. NREM sleep was defined as synchronized, high-amplitude, low-frequency EEG and substantially reduced EMG activity compared with wakefulness, with no phasic bursts. REM sleep was defined as having a pronounced theta rhythm (5-9 Hz) with no EMG activity. The first epoch during which a pronounced theta rhythm was detected, together with reduced EEG amplitude and EMG integral, was defined as the epoch of NREM to REM transition. For all further EEG data analyses, raw (not filtered) EEG/EMG data was exported from the sleep analysis software (SleepSign for Animal) and imported into Matlab using a custom script. To estimate EEG power in a specific band we filtered the EEG in that band and took the absolute value of the Hilbert transform of the filtered trace.

eNeuro Accepted Manuscript

Salient stimuli presentation

We gently introduced salient stimuli to the home cage of test mice that were individually housed and connected to fiber optic and EEG/EMG recording cables. In each experimental session, each test mouse was exposed to one stimulus (n = 4-5 per stimulus). Different stimuli were presented several days apart. Salient stimuli were: (1) 8 to 12 weeks-old female C57BL/6J mice (Jackson Laboratory), (2) ex-breeder CD1 male mice (>4 month old), (3) 4-weeks-old male C57BL/6J mice, (4) high-fat chow (D12451, Research Diets, Inc.); and (5) rat bedding. We provided test mice with a small piece (0.3 g) of high-fat chow during the two days preceding the high-fat chow experiment. We recorded fiber photometry and EEG/EMG signal prior to and following the introduction of the salient stimuli.

Immunohistochemistry

Following completion of experiments, mice were deeply anesthetized with ketamine and xylazine (100 and 20 mg kg−1, respectively, i.p.) and transcardially perfused with 1× PBS followed by 4% paraformaldehyde (PFA) in PBS. Brains were removed and post-fixed overnight in 4% PFA. Brains were then cryoprotected in 30% sucrose for minimum 48 h at 4 °C, and then sectioned (30 µm) on a cryostat (Leica Microsystems), collected in PBS containing 0.1% NaN_3 and stored at 4 °C.

Sections underwent immunohistochemical staining as described below. Primary antibodies were used at 1:1,000 dilution: chicken anti-tyrosine hydroxylase (#TYH, Aves Labs, Inc.) and rabbit anti-GABA (#20094, IMMUNOSTAR). Immunofluorescent

eNeuro Accepted Manuscript

secondary antibodies were used at 1:500 dilution: donkey anti-chicken Alexa Fluor 594 (#703-585-155, Jackson ImmunoResearch Laboratories, Inc.) for GCaMP6 and TH co-localization, and donkey anti-rabbit Alexa Fluor 594 (#711-585-152, Jackson ImmunoResearch Laboratories, Inc.) for GCaMP6 and GABA co-localization.

For immunofluorescence staining, brain sections were washed in PBS for 5 min and then incubated in a blocking solution composed of PBS with 0.3% Triton X-100 (PBST) containing 4% bovine serum albumin for 1 h. Sections were then incubated for ~16 h in block solution containing primary antibodies. After three 5-min washes in PBS, sections were incubated in blocking solution for 1 h and then incubated for 2 h in blocking solution containing secondary antibodies. Sections were washed three times for 5 min each in PBS, mounted onto gelatin-coated microscope slides (FD Neurotechnologies, #PO101) and coverslipped with Fluoroshield containing DAPI Mounting Media (Sigma, #F6057).

Microscopy and image analysis.

Images were collected on a Zeiss LSM 710 confocal fluorescent microscope using reflected light. Digital images were minimally processed using ImageJ (NIH) to enhance brightness and contrast for optimal representation.

Statistical analyses

Sample sizes were chosen based upon previous publications for the study of the sleep-wake circuitry. We used two-way RM ANOVAs for analyses of calcium signal and transient rate (Figs 1E,G and 6f; Factor 1: 'Mice', Factor 2: 'Arousal state'). We used

eNeuro Accepted Manuscript

two-tailed paired t-test's for data presented in Figures 1F,H. To correct for the multiple comparisons in these analyses we used a Bonferroni correction, i.e. we multiplied the obtained p-values by the number of comparisons (x 3). We used correlation coefficient to determine the correlation between fluorescence and power in specific frequency bands (Figs. 3-5). To correct for the multiple comparisons in the analyses of correlation between fluorescence and power in specific frequency bands we used a Bonferroni correction, and multiplied the obtained p-values by the number of comparisons (Wake, x2 (theta and gamma comparisons); NREM, x3 (delta, theta and sigma comparisons); REM, x2 (theta and gamma comparisons)). We analyzed data using Prism 6.0 (GraphPad Software) and Matlab R2016b software. Data are presented as mean ± s.e.m. unless otherwise indicated. For the preparation of the figures, we used Matlab R2016b and Prism 6.0 and then exported the data into Adobe Illustrator CS6 (Adobe Systems).

Results

VTA-GABAergic neuronal activity is modulated across arousal state

To assess population activity of VTA-GABAergic neurons across spontaneous sleep-wake states we used calcium-based fiber photometry recordings (**Fig. 1A-C**). We injected a Cre-dependent adeno-associated virus (AAV) encoding the fluorescent calcium indicator GCaMP6s (pAAV-DJ-EF1α-DIO-GCamP6s) into the VTA of Vgat-IRES-Cre knock-in mice and implanted a fiber optic probe above the VTA for

eNeuro Accepted Manuscript

subsequent delivery of excitation light and collection of fluorescent emission and with EEG-EMG electrodes for simultaneous sleep-wake recordings. Fluorescent immunostaining for GABA and tyrosine hydroxylase (TH) in GCaMP6-expressing slices demonstrated specific co-expression of GCaMP6 in GABAergic, but not dopaminergic VTA neurons (**Fig. 1A)**. We found robust alterations in both fluorescence signal (%ΔF/F) and calcium transient rate (Hz) in VTA-GABAergic neurons over spontaneous sleep/wake states (**Fig. 1D-H**). During NREM sleep, VTA-GABAergic neurons showed the lowest fluorescence and calcium transient rates compared to both wakefulness and REM sleep (**Fig. 1D-H**). In contrast, VTA-GABAergic neurons showed the most frequent calcium transients during REM sleep compared to both wakefulness and NREM sleep (**Fig. 1G-H**). These arousal-state-dependent alterations in activity were not found in control experiments (**data not shown**).

We proceeded to determine whether activity in VTA-GABAergic neurons is altered around arousal-state transitions. VTA-GABAergic neurons showed a strong decrease in population activity at wake to NREM transitions (**Fig. 2A-B**), while EEG delta power was strongly increased (**Fig. 2C**). These alterations were not found in control experiments (**data not shown**). NREM sleep to wakefulness transitions were accompanied by a large increase in population activity and a decrease in EEG delta power (**Fig. 2A-C**), even for short (<12 sec) wake episodes (**data not shown**). During NREM to REM sleep transitions, the $\Delta F/F$ signal showed a gradual ramping 10-20 seconds prior to the vigilance state transition, subsequently peaking ~20 seconds following the transition (**Fig. 2A,B**). Following REM sleep to wake transitions, a reduction in VTA-GABAergic calcium fluorescence was observed (**Fig. 2A,B**). Together, these findings demonstrate

eNeuro Accepted Manuscript

that VTA-GABAergic neurons exhibit strong alterations in population activity across arousal states.

VTA-GABAergic neuronal activity correlates with specific cortical oscillatory patterns

To investigate whether VTA-GABAergic neural activity is correlated with specific components of the EEG during different vigilance states, we examined correlations between population activity and power within specific EEG bands during 1-sec epochs of wakefulness, NREM, and REM sleep. During wakefulness, we found a negative correlation between VTA-GABAergic population activity and EEG theta (5-9 Hz) power, and a positive correlation of population activity and EEG gamma (30-80 Hz) power (**Fig. 3A,B**; Theta: $R(19,730) = -0.18$, $P < 0.0001$; Gamma: $R(19,730) = 0.33$, $P < 0.0001$). The positive gamma correlation was evident across all test mice, and was absent in control experiments (**data not shown**). In contrast, population activity of VTA-dopaminergic neurons was not correlated with the EEG gamma band, and only weakly correlated with theta (**Fig. 4A,B;** Theta: $R(12,884) = -0.05$, $P < 0.0001$; Gamma: $R(12,884) = 0.01$, $P = 0.1$). These data suggest that during wakefulness, activity of VTA-GABAergic, but not dopaminergic, neurons is related to fast cortical oscillations.

During NREM sleep, we observed a negative correlation between VTA-GABAergic population activity and EEG delta (1-4.5 Hz), theta and sigma (10-14 Hz) power bands (**Fig. 3C-E;** $R(43,810) = -0.04$ (Delta), -0.12 (Theta) and -0.15 (Sigma), $P < 0.0001$). Moreover, power in these frequency bands was significantly lower during high $\Delta F/F$ times as compared to low $\Delta F/F$ times (**data not shown**). Similar to VTA-GABAergic

eNeuro Accepted Manuscript

neurons, VTA-dopaminergic neurons showed a negative correlation between population activity and EEG delta, theta, and sigma power bands during NREM sleep (**Fig. 4C-E;** R(33,467) = -0.06 (Delta), -0.07 (Theta) and -0.07 (Sigma), P < 0.0001). Together our findings suggest that within NREM sleep, high activity periods in both VTA-GABAergic and VTA-dopaminergic neurons are associated with a lightening of NREM sleep.

Within REM sleep, we found a significant, yet weak, negative correlation between VTA-GABAergic population activity and both EEG theta and gamma power bands (**Fig. 3F,G;** R(43,810) = -0.06 (Gamma) and -0.05 (Theta), P < 0.0001). In contrast, VTA-dopaminergic neurons showed an opposite, yet weak, trend for EEG theta power and no correlation for EEG gamma power (**Fig. 4D,E**).

We also determined the correlation between VTA-GABAergic neural activity and specific components of the EEG across arousal states. We found that VTA-GABAergic population activity is negatively correlated to delta, theta and sigma power bands (R(71,926) = -0.3 (Delta), -0.31 (Theta) and -0.34 (Sigma), P < 0.0001) and positively correlated with EEG gamma power (R(71,926) = 0.13, P < 0.0001). Taken together, our findings demonstrate that activity in VTA-GABAergic neurons is strongly associated with both behavioral and electrocortical arousal.

VTA-GABAergic neurons exhibit biased responses to social stimuli

To further explore the relationship between activity in VTA-GABAergic neurons and arousal, we presented mice with various salient stimuli, of both positive and negative

eNeuro Accepted Manuscript

valences, while simultaneously recording population activity from VTA-GABAergic neurons and EEG/EMG signals. Following the placement of salient stimuli inside the home cage of test mice, VTA-GABAergic neurons showed a fast increase in population activity (**Fig. 5A-E**). Social stimuli (female mouse, juvenile mouse and an aggressive mouse) induced an increase in activity that remained elevated for more than 120 seconds, irrespective of valence (**Fig. 5A-C**). Non-social salient stimuli, associated with both positive (high fat chow) and negative (rat bedding) valences, induced much weaker activation of VTA-GABAergic neurons (**Fig. 5D-F**). As during spontaneous wakefulness, population activity of VTA-GABAergic neurons showed a positive correlation with EEG gamma power during the presentation of most salient stimuli (**Fig. 5G-K**). Surprisingly, no correlation between population activity of VTA-GABAergic neurons and EEG gamma power was found during trials in which male mice were presented (both young and older/aggressive males) (**Fig. 5G-K**). Together, these findings further support the premise that VTA-GABAergic neurons activity is tightly linked to behavioral and electrocortical arousal.

Discussion

Here, we investigated the relationships between electrocortical and behavioral arousal and population activity of subsets of neurons in the VTA. We observed that activity in VTA-GABAergic neurons varies significantly across arousal states. VTA-GABAergic neurons are strongly activated during wakefulness and REM sleep and show low population activity during NREM sleep. Moreover, during NREM sleep, population

eNeuro Accepted Manuscript

activity of VTA-GABAergic neurons negatively correlates with NREM sleep intensity, i.e. delta, theta and sigma power bands. In contrast, during wakefulness population activity of VTA-GABAergic neurons is positively correlated with EEG gamma power. We also found that VTA-GABAergic neurons are strongly activated by different salient stimuli, specifically social stimuli of both positive and negative valence. Activity of VTA-dopaminergic neurons was found to be similarly negatively correlated with NREM sleep intensity but, notably, we did not observe a significant correlation between population activity and gamma power during wakefulness. Together, our findings demonstrate that the VTA, which is mainly studied in regard to reward, motivation and learning, also shows strong modulation by arousal state.

Both VTA dopaminergic and GABAergic neurons are strongly activated by rewards and reward-predictive cues, yet VTA-GABAergic neurons show sustained excitation following a reward-predictive cue while activity in VTA-dopaminergic neurons is suppressed in the delay period between cue and reward delivery (Cohen et al., 2012). It has been suggested that sustained activation of VTA-GABAergic neurons during the delay period accounts for the suppression of VTA-dopaminergic neural activity and possibly the computation of reward prediction error (Schultz, 1998; Cohen et al., 2012). VTA-GABAergic neurons inhibit VTA-dopaminergic neurons both *in vitro* (Dobi et al., 2010; van Zessen et al., 2012) and in anesthetized rats (Tan et al., 2012). It has been proposed that VTA-GABAergic neurons do not exert a tonic inhibition on VTA-dopaminergic neurons, but rather sculpt their activity pattern in favor of fast oscillations (Brown and McKenna, 2015). In the context of sleep/wake regulation, we have previously demonstrated that VTA-dopaminergic neurons increase their activity

eNeuro Accepted Manuscript

prior to NREM sleep-to-wake transitions (Eban-Rothschild et al., 2016), while here we report that VTA-GABAergic neurons increase their activity in conjunction with these transitions (Fig. 2). It is thus unlikely that VTA-GABAergic neurons drive NREM sleep-to-wake transitions. Rather, VTA-GABAergic neurons may suppress activity in VTA-dopaminergic neurons following a sleep-to-wake transition–to tightly control arousal. Indeed, lesioning or chemogenetic inhibition of VTA-GABAergic neurons produces persistent wakefulness (Takata et al., 2018; Yu et al., 2019b). VTA-dopaminergic neural activation potently promotes arousal and maintains long-term wakefulness (Eban-Rothschild et al., 2016; Taylor et al., 2016; Oishi et al., 2017), and the increased activity in VTA-dopaminergic neurons suppresses the motivation to prepare for sleep and engage in sleep-preparatory behaviors (Eban-Rothschild et al., 2016). It is reasonable to assume that activity in VTA-dopaminergic neurons is tightly regulated to suppress wakefulness when sleep is in need and prevent a state of hyperarousal (Yu et al., 2019a)–as may be the case in mania or drug-induced arousal. Cocaine, for example, reduces activity in VTA-GABAergic neurons, which results in disinhibition of VTA-dopaminergic neurons and the elevation of extracellular dopamine concentrations (Bocklisch et al., 2013). Similarly, optogenetic inhibition of VTA-GABAergic neurons results in disinhibition of VTA-dopaminergic neurons and an increase in VTA-dopaminergic neuronal activation (Bocklisch et al., 2013). Together, our findings provide a mechanistic framework for the participation of dopaminergic and GABAergic VTA neurons in the regulation of arousal. A better understanding of VTA microcircuitry in the context of arousal regulation holds great promise to improve

eNeuro Accepted Manuscript

448 the capacity to treat sleep dysregulation in pathological circumstances, such as drug
449 addiction.

450 It is important to mention that in the current study we did not distinguish between
451 subpopulations of GABAergic neurons. For example, some VTA-GABAergic neurons
452 express corticotropin-releasing factor (CRF)-binding protein (Wang and Morales, 2008),
453 dopamine receptor D2, or μ-opioid receptors (Margolis et al., 2012). In addition, some
454 VTA-GABAergic interneurons form local connections within the VTA while others send
455 long-range projections (Morales and Margolis, 2017). It would be of interest for future
456 studies to determine whether these disparate populations differentially influence
457 arousal. Recently, Yu and colleagues made progress in this regard. They
458 demonstrated that VTA-GABAergic neurons project to the lateral hypothalamus,
459 where they inhibit wakefulness and drive NREM sleep (Yu et al., 2019b). When VTA-
460 GABAergic neural activity was monitored using fiber photometry, they observed high
461 calcium fluorescence during wakefulness and REM sleep, similar to our findings. In
462 contrast, Chowdhury and colleagues recently observed that GAD67+ GABAergic
463 neurons in the VTA are mostly active during NREM sleep (Chowdhury et al., 2019).
464 The discrepancy between the different studies may be due to the use of a different
465 Cre-line to target GABAergic neurons in the VTA (Vgat-cre vs. GAD67-cre), or to the
466 targeting of different VTA sub-regions. While Yu et al. and our study targeted relatively
467 rostral regions of the VTA (3.3 mm posterior to Bregma) Chowdhury et al. may have
468 targeted caudal regions of the VTA (3.0-3.7 mm posteriorly to Bregma). Indeed,
469 GABAergic neurons in the tail of the VTA, or RMTg, have been demonstrated to
470 promote NREM sleep via inhibition of VTA dopaminergic neurons (Yang et al., 2018).

eNeuro Accepted Manuscript

The different studies (Yu et al., Chowdhury et al. and Eban-Rothschild et al.) also used different viral constructs and/or promoters that may have influenced the viral tropism and expression levels of GCaMP in the VTA. It is also important to note that while Chowdhury and colleagues reported higher population activity in VTA GAD67+ neurons during NREM sleep compared to wakefulness and REM sleep, examination of their data suggests an increase in population activity immediately following sleep-to-wake transitions, and higher transient rates during wakefulness and REM sleep compared to NREM sleep (Chowdhury et al., 2019). Broadly, GABAergic neurons are highly heterogeneous across the brain (e.g., see (Jones, 2017)), and the use of bulk population activity recordings may mask ensemble differences in activity patterns. Nonetheless, using microendoscope calcium imaging of VTA-GABAergic neurons Yu and colleagues reported a similar Wake on/NREM off activity pattern, although their sample size was relatively low (Yu et al., 2019b). Further research is needed to tease apart how specific subsets of VTA-GABAergic neurons contribute to arousal state regulation.

How are VTA-GABAergic neurons linked to other sleep/wake regulatory centers? VTA-GABAergic neurons receive excitatory, inhibitory and modulatory inputs from diverse cortical and subcortical areas (Beier et al., 2015; Faget et al., 2016). Putative VTA-GABAergic neurons are strongly activated by different arousal-related neuromodulators including hypocretin, CRF, substance P, and histamine (Korotkova et al., 2002; Korotkova et al., 2006). VTA-GABAergic neurons send widespread projections to various forebrain and brainstem areas including the basal forebrain, lateral hypothalamus, periaqueductal gray and dorsal raphe nuclei, as well as sparser

eNeuro Accepted Manuscript

494 projections to the nucleus accumbens and prefrontal cortex (Carr and Sesack, 2000b;
495 Kirouac et al., 2004; Brown et al., 2012; van Zessen et al., 2012; Taylor et al., 2014).
496 Together these observations demonstrate that VTA-GABAergic neurons are well
497 positioned to regulate local and global neuronal activity for the support of
498 electrocortical and behavioral arousal.

499 We found that VTA-GABAergic neural activity correlated with specific components of
500 the EEG power spectrum. Across arousal states, delta, theta and sigma power bands
501 were negatively correlated with VTA-GABAergic activity (Fig. 3). Slow oscillations in the
502 EEG are related to the depth of sleep, correlate with the duration of prior waking, and
503 are a signature of widespread synchronization of cortical and thalamo-cortical networks
504 (Contreras et al., 1996; Cirelli, 2009; Borbely et al., 2016). Sleep spindles, periodic
505 oscillatory patterns in the NREM EEG that overlap with the sigma power band (10-14
506 Hz), are thought to stabilize sleep and promote memory consolidation (Mednick et al.,
507 2013; Rasch and Born, 2013). Spindles are primarily generated by the thalamic reticular
508 nucleus (RTN), where GABAergic neurons function as a pacemaker, and glutamatergic
509 thalamo-cortical projections mediate the propagation of spindles to the cortex (von
510 Krosigk et al., 1993; Contreras et al., 1996; De Gennaro and Ferrara, 2003). A similar
511 pattern was observed for VTA-dopaminergic neurons, where high activity within this
512 population was negatively correlated with EEG delta, theta and sigma bands during
513 NREM sleep. Negative correlations between VTA neural activity and cortical NREM
514 sleep characteristics suggest that the concerted activity of these neurons may
515 fundamentally oppose slow oscillations. This may underlie chronic sleep disturbances in

eNeuro Accepted Manuscript

people who abuse drugs targeting the dopaminergic system (e.g., cocaine, methamphetamine).

We also found that activity in VTA-GABAergic, but not dopaminergic neurons, is positively correlated with EEG gamma power during both spontaneous and motivated wakefulness (Fig. 3-5). A previous study demonstrated that activity in the VTA and prefrontal cortex (PFC) is coupled via a 4 Hz oscillation that synchronizes local gamma oscillations and neuronal firing (Fujisawa and Buzsaki, 2011). Moreover, the authors reported a task-dependent increase in gamma coherence between the PFC and the VTA during a working memory task (Fujisawa and Buzsaki, 2011). The cellular identity in the VTA accounting for this coupling remained elusive (Fujisawa and Buzsaki, 2011). VTA-GABAergic neurons both receive input from and send reciprocal projections to the PFC (Carr and Sesack, 2000b, a). It is possible that the strong correlation between VTA-GABAergic activation and EEG gamma oscillations reflects a top-down cognitive process via transmission of information from the PFC to fast-spiking VTA-GABAergic neurons. Cortical gamma band activity is largely generated by fast-spiking GABAergic parvalbumin positive interneurons (Sohal et al., 2009), and is hypothesized to enhance information processing and attention (Womelsdorf et al., 2007). VTA-GABAergic activity may also be related to cortical processes associated with gamma activity, such as the temporal representation and consolidation of information (Buzsaki and Draguhn, 2004). Interestingly, our findings suggest that not all behaviors are characterized by this gamma coupling, including interactions with same sex conspecifics. Indeed, further studies using projection-specific manipulations could add valuable insights to the

eNeuro Accepted Manuscript

538 functional role of VTA-GABAergic neural activity and their relation to cortical gamma
539 oscillations.

540 Lastly, we observed strong and enduring calcium responses from VTA-GABAergic
541 neurons during the presentation of social stimuli. Specifically, large increases in
542 neuronal activity were observed in response to a novel female mouse, aggressive male
543 intruder, and a 4-week old juvenile mouse, suggesting that population-level VTA-
544 GABAergic responses to social stimuli are independent of valence. In contrast, we
545 observed significantly smaller responses to both positive (high fat diet) and negative (rat
546 bedding) stimuli that did not involve a social novelty component. It is important to note
547 that we did not control for possible motor aspects of social stimuli. Although Lee et al.
548 demonstrated that the firing rate of VTA-GABAergic neurons was phasically modulated
549 by certain movements, such as head orienting, little variation in firing rate was observed
550 during sustained locomotor activity (Lee et al., 2001). VTA neurons, specifically
551 dopaminergic, are associated with social reward and social novelty (Gunaydin et al.,
552 2014; Hung et al., 2017), yet the precise function of VTA-GABAergic neurons in this
553 regard awaits further investigation.

554 In summary, we demonstrated that VTA-GABAergic neural activity is strongly
555 modulated by arousal state. As many addictive drugs inhibit VTA-GABAergic neurons,
556 resulting in VTA dopaminergic disinhibition (Hyman et al., 2006; Luscher and Malenka,
557 2011) a better understanding of VTA microcircuitry in arousal regulation may lead to
558 novel treatments for diseases involving disorders of cortical activation, hyper-arousal,
559 and disrupted sleep.

eNeuro Accepted Manuscript

References

Beier KT, Steinberg EE, DeLoach KE, Xie S, Miyamichi K, Schwarz L, Gao XJ, Kremer EJ, Malenka RC, Luo L (2015) Circuit Architecture of VTA Dopamine Neurons Revealed by Systematic Input-Output Mapping. Cell 162:622-634.

Berke JD (2018) What does dopamine mean? Nature neuroscience 21:787-793.

Berridge KC (2007) The debate over dopamine's role in reward: the case for incentive salience. Psychopharmacology 191:391-431.

Bocklisch C, Pascoli V, Wong JC, House DR, Yvon C, de Roo M, Tan KR, Luscher C (2013) Cocaine disinhibits dopamine neurons by potentiation of GABA transmission in the ventral tegmental area. Science (New York, NY) 341:1521-1525.

Borbely AA, Daan S, Wirz-Justice A, Deboer T (2016) The two-process model of sleep regulation: a reappraisal. Journal of sleep research 25:131-143.

Brown MT, Tan KR, O'Connor EC, Nikonenko I, Muller D, Luscher C (2012) Ventral tegmental area GABA projections pause accumbal cholinergic interneurons to enhance associative learning. Nature 492:452-456.

Brown RE, McKenna JT (2015) Turning a Negative into a Positive: Ascending GABAergic Control of Cortical Activation and Arousal. Frontiers in neurology 6:135.

Buzsaki G, Draguhn A (2004) Neuronal oscillations in cortical networks. Science (New York, NY) 304:1926-1929.

Carr DB, Sesack SR (2000a) Projections from the rat prefrontal cortex to the ventral tegmental area: target specificity in the synaptic associations with mesoaccumbens and mesocortical neurons. The Journal of neuroscience : the official journal of the Society for Neuroscience 20:3864-3873.

Carr DB, Sesack SR (2000b) GABA-containing neurons in the rat ventral tegmental area project to the prefrontal cortex. Synapse (New York, NY) 38:114-123.

Chowdhury S, Matsubara T, Miyazaki T, Ono D, Fukatsu N, Abe M, Sakimura K, Sudo Y, Yamanaka A (2019) GABA neurons in the ventral tegmental area regulate non-rapid eye movement sleep in mice. eLife 8.

Cirelli C (2009) The genetic and molecular regulation of sleep: from fruit flies to humans. Nature reviews Neuroscience 10:549-560.

Cohen JY, Haesler S, Vong L, Lowell BB, Uchida N (2012) Neuron-type-specific signals for reward and punishment in the ventral tegmental area. Nature 482:85-88.

Contreras D, Destexhe A, Sejnowski TJ, Steriade M (1996) Control of spatiotemporal coherence of a thalamic oscillation by corticothalamic feedback. Science (New York, NY) 274:771-774.

Dahan L, Astier B, Vautrelle N, Urbain N, Kocsis B, Chouvet G (2007) Prominent burst firing of dopaminergic neurons in the ventral tegmental area during paradoxical sleep. Neuropsychopharmacology : official publication of the American College of Neuropsychopharmacology 32:1232-1241.

De Gennaro L, Ferrara M (2003) Sleep spindles: an overview. Sleep medicine reviews 7:423-440.

Dobi A, Margolis EB, Wang HL, Harvey BK, Morales M (2010) Glutamatergic and nonglutamatergic neurons of the ventral tegmental area establish local synaptic contacts

eNeuro Accepted Manuscript

603 with dopaminergic and nondopaminergic neurons. The Journal of neuroscience : the
604 official journal of the Society for Neuroscience 30:218-229.
605 Eban-Rothschild A, Appelbaum L, de Lecea L (2018) Neuronal Mechanisms for Sleep/Wake
606 Regulation and Modulatory Drive. Neuropsychopharmacology : official publication of
607 the American College of Neuropsychopharmacology 43:937-952.
608 Eban-Rothschild A, Rothschild G, Giardino WJ, Jones JR, de Lecea L (2016) VTA
609 dopaminergic neurons regulate ethologically relevant sleep-wake behaviors. Nature
610 neuroscience 19:1356-1366.
611 Faget L, Osakada F, Duan J, Ressler R, Johnson AB, Proudfoot JA, Yoo JH, Callaway EM,
612 Hnasko TS (2016) Afferent Inputs to Neurotransmitter-Defined Cell Types in the Ventral
613 Tegmental Area. Cell reports 15:2796-2808.
614 Fifel K, Meijer JH, Deboer T (2018) Circadian and Homeostatic Modulation of Multi-Unit
615 Activity in Midbrain Dopaminergic Structures. Scientific reports 8:7765.
616 Fujisawa S, Buzsaki G (2011) A 4 Hz oscillation adaptively synchronizes prefrontal, VTA, and
617 hippocampal activities. Neuron 72:153-165.
618 Gomperts SN, Kloosterman F, Wilson MA (2015) VTA neurons coordinate with the
619 hippocampal reactivation of spatial experience. eLife 4.
620 Gunaydin LA, Grosenick L, Finkelstein JC, Kauvar IV, Fenno LE, Adhikari A, Lammel S,
621 Mirzabekov JJ, Airan RD, Zalocusky KA, Tye KM, Anikeeva P, Malenka RC,
622 Deisseroth K (2014) Natural neural projection dynamics underlying social behavior. Cell
623 157:1535-1551.
624 Hung LW, Neuner S, Polepalli JS, Beier KT, Wright M, Walsh JJ, Lewis EM, Luo L, Deisseroth
625 K, Dolen G, Malenka RC (2017) Gating of social reward by oxytocin in the ventral
626 tegmental area. Science (New York, NY) 357:1406-1411.
627 Hyman SE, Malenka RC, Nestler EJ (2006) Neural mechanisms of addiction: the role of reward-
628 related learning and memory. Annual review of neuroscience 29:565-598.
629 Jones BE (2017) Principal cell types of sleep-wake regulatory circuits. Current opinion in
630 neurobiology 44:101-109.
631 Kirouac GJ, Li S, Mabrouk G (2004) GABAergic projection from the ventral tegmental area and
632 substantia nigra to the periaqueductal gray region and the dorsal raphe nucleus. The
633 Journal of comparative neurology 469:170-184.
634 Korotkova TM, Haas HL, Brown RE (2002) Histamine excites GABAergic cells in the rat
635 substantia nigra and ventral tegmental area in vitro. Neuroscience letters 320:133-136.
636 Korotkova TM, Brown RE, Sergeeva OA, Ponomarenko AA, Haas HL (2006) Effects of
637 arousal- and feeding-related neuropeptides on dopaminergic and GABAergic neurons in
638 the ventral tegmental area of the rat. The European journal of neuroscience 23:2677-
639 2685.
640 Lammel S, Hetzel A, Hackel O, Jones I, Liss B, Roeper J (2008) Unique properties of
641 mesoprefrontal neurons within a dual mesocorticolimbic dopamine system. Neuron
642 57:760-773.
643 Lee RS, Steffensen SC, Henriksen SJ (2001) Discharge profiles of ventral tegmental area GABA
644 neurons during movement, anesthesia, and the sleep-wake cycle. The Journal of
645 neuroscience : the official journal of the Society for Neuroscience 21:1757-1766.
646 Lerner TN, Shilyansky C, Davidson TJ, Evans KE, Beier KT, Zalocusky KA, Crow AK,
647 Malenka RC, Luo L, Tomer R, Deisseroth K (2015) Intact-Brain Analyses Reveal
648 Distinct Information Carried by SNc Dopamine Subcircuits. Cell 162:635-647.

eNeuro Accepted Manuscript

649 Luscher C, Malenka RC (2011) Drug-evoked synaptic plasticity in addiction: from molecular
650 changes to circuit remodeling. Neuron 69:650-663.
651 Maloney KJ, Mainville L, Jones BE (2002) c-Fos expression in dopaminergic and GABAergic
652 neurons of the ventral mesencephalic tegmentum after paradoxical sleep deprivation and
653 recovery. The European journal of neuroscience 15:774-778.
654 Margolis EB, Lock H, Hjelmstad GO, Fields HL (2006) The ventral tegmental area revisited: is
655 there an electrophysiological marker for dopaminergic neurons? The Journal of
656 physiology 577:907-924.
657 Margolis EB, Toy B, Himmels P, Morales M, Fields HL (2012) Identification of Rat Ventral
658 Tegmental Area GABAergic Neurons. PloS one 7:e42365.
659 Mednick SC, McDevitt EA, Walsh JK, Wamsley E, Paulus M, Kanady JC, Drummond SP
660 (2013) The critical role of sleep spindles in hippocampal-dependent memory: a
661 pharmacology study. The Journal of neuroscience : the official journal of the Society for
662 Neuroscience 33:4494-4504.
663 Miller JD, Farber J, Gatz P, Roffwarg H, German DC (1983) Activity of mesencephalic
664 dopamine and non-dopamine neurons across stages of sleep and walking in the rat. Brain
665 research 273:133-141.
666 Morales M, Margolis EB (2017) Ventral tegmental area: cellular heterogeneity, connectivity and
667 behaviour. Nature reviews Neuroscience 18:73-85.
668 Nair-Roberts RG, Chatelain-Badie SD, Benson E, White-Cooper H, Bolam JP, Ungless MA
669 (2008) Stereological estimates of dopaminergic, GABAergic and glutamatergic neurons
670 in the ventral tegmental area, substantia nigra and retrorubral field in the rat.
671 Neuroscience 152:1024-1031.
672 Oishi Y, Suzuki Y, Takahashi K, Yonezawa T, Kanda T, Takata Y, Cherasse Y, Lazarus M
673 (2017) Activation of ventral tegmental area dopamine neurons produces wakefulness
674 through dopamine D2-like receptors in mice. Brain Struct Funct 222:2907-2915.
675 Rasch B, Born J (2013) About sleep's role in memory. Physiological reviews 93:681-766.
676 Salamone JD, Correa M (2012) The mysterious motivational functions of mesolimbic dopamine.
677 Neuron 76:470-485.
678 Schultz W (1998) Predictive Reward Signal of Dopamine Neurons. Journal of neurophysiology
679 80:1-27.
680 Sohal VS, Zhang F, Yizhar O, Deisseroth K (2009) Parvalbumin neurons and gamma rhythms
681 enhance cortical circuit performance. Nature 459:698-702.
682 Steinfels GF, Heym J, Strecker RE, Jacobs BL (1983) Behavioral correlates of dopaminergic unit
683 activity in freely moving cats. Brain research 258:217-228.
684 Takata Y, Oishi Y, Zhou XZ, Hasegawa E, Takahashi K, Cherasse Y, Sakurai T, Lazarus M
685 (2018) Sleep and wakefulness are controlled by ventral medial midbrain/pons
686 GABAergic neurons in mice. The Journal of neuroscience : the official journal of the
687 Society for Neuroscience.
688 Tan KR, Yvon C, Turiault M, Mirzabekov JJ, Doehner J, Labouebe G, Deisseroth K, Tye KM,
689 Luscher C (2012) GABA neurons of the VTA drive conditioned place aversion. Neuron
690 73:1173-1183.
691 Taylor NE, Van Dort CJ, Kenny JD, Pei J, Guidera JA, Vlasov KY, Lee JT, Boyden ES, Brown
692 EN, Solt K (2016) Optogenetic activation of dopamine neurons in the ventral tegmental
693 area induces reanimation from general anesthesia. Proceedings of the National Academy
694 of Sciences 113:12826-12831.

eNeuro Accepted Manuscript

Taylor SR, Badurek S, Dileone RJ, Nashmi R, Minichiello L, Picciotto MR (2014) GABAergic and glutamatergic efferents of the mouse ventral tegmental area. The Journal of comparative neurology 522:3308-3334.
Ungless MA, Grace AA (2012) Are you or aren't you? Challenges associated with physiologically identifying dopamine neurons. Trends in neurosciences 35:422-430.
van Zessen R, Phillips JL, Budygin EA, Stuber GD (2012) Activation of VTA GABA neurons disrupts reward consumption. Neuron 73:1184-1194.
von Krosigk M, Bal T, McCormick DA (1993) Cellular mechanisms of a synchronized oscillation in the thalamus. Science (New York, NY) 261:361-364.
Wang HL, Morales M (2008) Corticotropin-releasing factor binding protein within the ventral tegmental area is expressed in a subset of dopaminergic neurons. The Journal of comparative neurology 509:302-318.
Womelsdorf T, Schoffelen JM, Oostenveld R, Singer W, Desimone R, Engel AK, Fries P (2007) Modulation of neuronal interactions through neuronal synchronization. Science (New York, NY) 316:1609-1612.
Yang SR, Hu ZZ, Luo YJ, Zhao YN, Sun HX, Yin D, Wang CY, Yan YD, Wang DR, Yuan XS, Ye CB, Guo W, Qu WM, Cherasse Y, Lazarus M, Ding YQ, Huang ZL (2018) The rostromedial tegmental nucleus is essential for non-rapid eye movement sleep. PLoS biology 16:e2002909.
Yu X, Ba W, Zhao G, Ma Y, Harding EC, Yin L, Wang D, Shi Y, Vyssotski AL, Dong H, Franks NP, Wisden W (2019a) Dysfunction of ventral tegmental area GABA neurons causes mania-like behavior. bioRxiv:684142.
Yu X, Li W, Ma Y, Tossell K, Harris JJ, Harding EC, Ba W, Miracca G, Wang D, Li L, Guo J, Chen M, Li Y, Yustos R, Vyssotski AL, Burdakov D, Yang Q, Dong H, Franks NP, Wisden W (2019b) GABA and glutamate neurons in the VTA regulate sleep and wakefulness. Nature neuroscience 22:106-119.

Figure Legends:

Figure 1: **VTA-GABAergic neurons show arousal-state dependent alterations in population activity**. (**A**) Confocal microscopic images of AAV-DJ-EF1α-DIO-GCaMP6s expression in the VTA co-immunostained with anti-GABA (top) or anti-TH (bottom) antibodies, demonstrating selective calcium indicator expression in VTA-GABAergic neurons, but not VTA-dopaminergic neurons. (**B**) Schematic for simultaneous recordings of VTA-GABA-GCaMP6s and EEG/EMG signals in *Vgat*-Cre mice. (**C**)

eNeuro Accepted Manuscript

Representative image of GCaMP6s-expressing neurons in the VTA and the fiber optic tract for recording. (**D**) Representative fluorescence trace color-coded by arousal state (wake, NREM and REM sleep). Identified transients are denoted by open circles. (**E**) Mean ± s.e.m. fluorescence during wake, NREM and REM sleep (two-way repeated-measures (RM) ANOVA between 'Mice' and 'Arousal state'. Mice, $F_{7,31} = 0.006$, $P > 0.99$. Arousal state, $F_{2,62} = 8.075$, $P = 0.0008$, followed by Tukey's *post hoc* tests, wake vs. NREM $P > 0.99$, wake vs. REM $P = 0.0027$, NREM vs. REM $P = 0.0027$). (**F**) Scatter plots comparing mean %ΔF/F values for pairs of arousal states (paired samples t-test's, Wake vs. NREM, t(38)= -9.8881, $P = 4.6 \times 10^{-12}$; REM vs. NREM, t(38)= -14.8166, $P = 2.2 \times 10^{-17}$; Wake vs. REM, t(38)= -6.387, $P = 1.68 \times 10^{-7}$). Each dot represents a single trial. The different colors represent different mice. (**G**) Transient rate (Hz) for wake, NREM and REM sleep (two-way repeated-measures (RM) ANOVA between 'Mice' and 'Arousal state'. Mice, $F_{7,31} = 0.7776$, $P = 0.61$. Arousal state, $F_{2,62} = 117.8$, $P < 1 \times 10^{-15}$, followed by Tukey's *post hoc* tests, wake vs. NREM = 4.39×10^{-10}, wake vs. REM $P = 3.99 \times 10^{-10}$, NREM vs. REM $P = 1.89 \times 10^{-11}$). (H) Scatter plots comparing mean transient rate values among each pair of arousal state (paired samples t-test's, Wake vs. NREM, t(38)= -10.2078, $P = 1.9 \times 10^{-12}$; REM vs. NREM, t(38)= -20.1677, $P = 6.7 \times 10^{-22}$; Wake vs. REM, t(38)= -6.3469, $P = 1.9 \times 10^{-7}$). Each dot represents a single trial. The different colors represent different mice.

Figure 2: **VTA-GABAergic population dynamics around arousal state transitions.** (**A**) Heatmaps of fluorescence intensity aligned to arousal state transitions (wake to NREM, $n = 459$; NREM to wake, $n = 329$; NREM to REM, $n = 135$; REM to wake, $n = 135$). Trials are sorted by the duration of the second state (shortest, top; longest,

eNeuro Accepted Manuscript

753 bottom). (**B**) Average responses from all the transitions expressed as mean (blue
754 trace) ± s.e.m. (gray shading). (**C**) EEG delta (1-4.5 Hz) power from all the transitions.

755 **Figure 3: VTA-GABAergic population activity is positively correlated with fast-**
756 **frequency EEG oscillations during wakefulness and negatively correlated with**
757 **low-frequency oscillations during NREM sleep.** Correlations between EEG spectral
758 components and population activity during spontaneous wakefulness (**A,B**), NREM
759 sleep (**C-E**), REM sleep (**F,G**) and across the 3 states (**H**). Each dot represents a 1-
760 second epoch. Dashed line is the best linear fit. R is correlation coefficient. Right panels
761 in each arousal state section represent a: representative raw EEG trace, fluorescence
762 trace, filtered EEG and power in a specific EEG band for a 2-10 seconds wake epoch.

763 **Figure 4: Correlations between EEG spectral components and VTA-dopaminergic**
764 **neural activity during wakefulness, NREM and REM sleep.** Correlations between
765 EEG spectral components and VTA-dopaminergic population activity during
766 spontaneous sleep/wake states. VTA-dopaminergic population activity plotted against
767 EEG theta (**A**) and gamma (**B**), power during wakefulness. VTA-dopaminergic
768 population activity plotted against EEG delta (**C**), theta (**D**) and sigma (**E**) power during
769 NREM sleep. VTA-dopaminergic population activity plotted against EEG theta (**F**) and
770 gamma (**G**) power during REM sleep. Each dot represents a 1-second epoch. Dashed
771 line is the best linear fit. R is correlation coefficient.

772 **Figure 5: VTA-GABAergic neurons are strongly activated by social salient stimuli.**
773 (**A-E**) Population activity of VTA-GABAergic neurons prior and following the placement
774 of (**A**) a female mouse, (**B**) an aggressive (CD1) male mouse, (**C**) a juvenile male

eNeuro Accepted Manuscript

mouse, (**D**) high fat rodent chow, and (**E**) rat bedding, inside the home cage of test mice. Presented are 60 seconds prior to and 120 seconds following stimulus presentation. (**F**) Summary data showing the relative change in %ΔF/F for each stimulus prior to and after presentations (two-way ANOVA: main effect of time $F_{1,19}$ = 95.92, $p < 0.0001$; main effect of stimuli $F_{4,19}$ = 5.324, $p = 0.0048$; and the interaction $F_{4,19}$ = 5.759, $p = 0.0033$). Sidak's multiple comparisons post-hoc tests reveal stimulus-specific responses in the %ΔF/F signal (no differences were observed during baseline prior to stimulus presentation; after stimulus presentation, female mouse vs. aggressive mouse $t = 0.8874$, $p > 0.05$, female mouse vs. juvenile male mouse $t = 0.8488$, $p > 0.05$, female mouse vs. high fat diet $t = 3.901$, $p = 0.0038$, female mouse vs. rat (predator) bedding $t = 4.391$, $p = 0.0009$, aggressive mouse vs. juvenile mouse $t = 1.736$, $p > 0.05$, aggressive mouse vs. high fat diet $t = 3.014$, $p = 0.0448$, aggressive mouse vs. rat bedding $t = 3.555$, $p = 0.0103$, juvenile mouse vs. high fat diet $t = 4.75$, $p = 0.0003$, juvenile mouse vs. rat bedding $t = 5.192$, $p < 0.0001$, high fat diet vs. rat bedding $t = 0.7133$, $p > 0.05$. Before and after stimulus comparisons further allow for specific effects of each stimulus to be assessed (Sidak's): female mouse $t = 5.983$, $p < 0.0001$, aggressive mouse $t = 5.459$, $p = 0.0001$, juvenile mouse $t = 7.249$, $p < 0.0001$, high fat diet $t = 2.474$, $p > 0.05$, rat bedding $t = 1.14$, $p > 0.05$. Note that before and after stimulus differences are only significant for social stimuli (female and male mice), but not for nonsocial stimuli (high fat chow and rat bedding). **(G-K)** Correlations between EEG gamma power and VTA-GABAergic neural activity following the presentation of salient stimuli. Each dot represents a 1-second epoch. Dashed line is the best linear fit. R is correlation coefficient.

eNeuro Accepted Manuscript

Figure 1

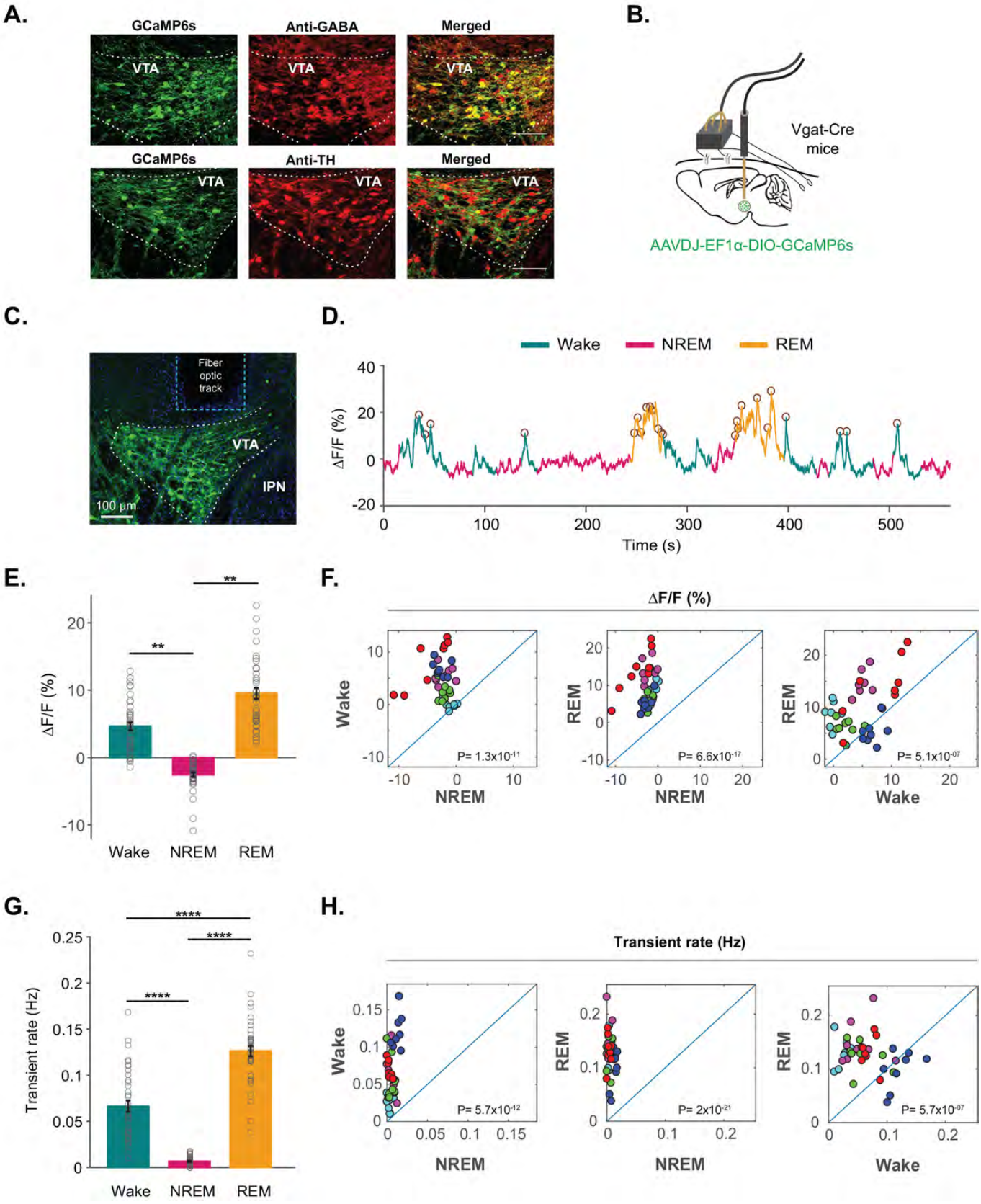

eNeuro Accepted Manuscript

Figure 2

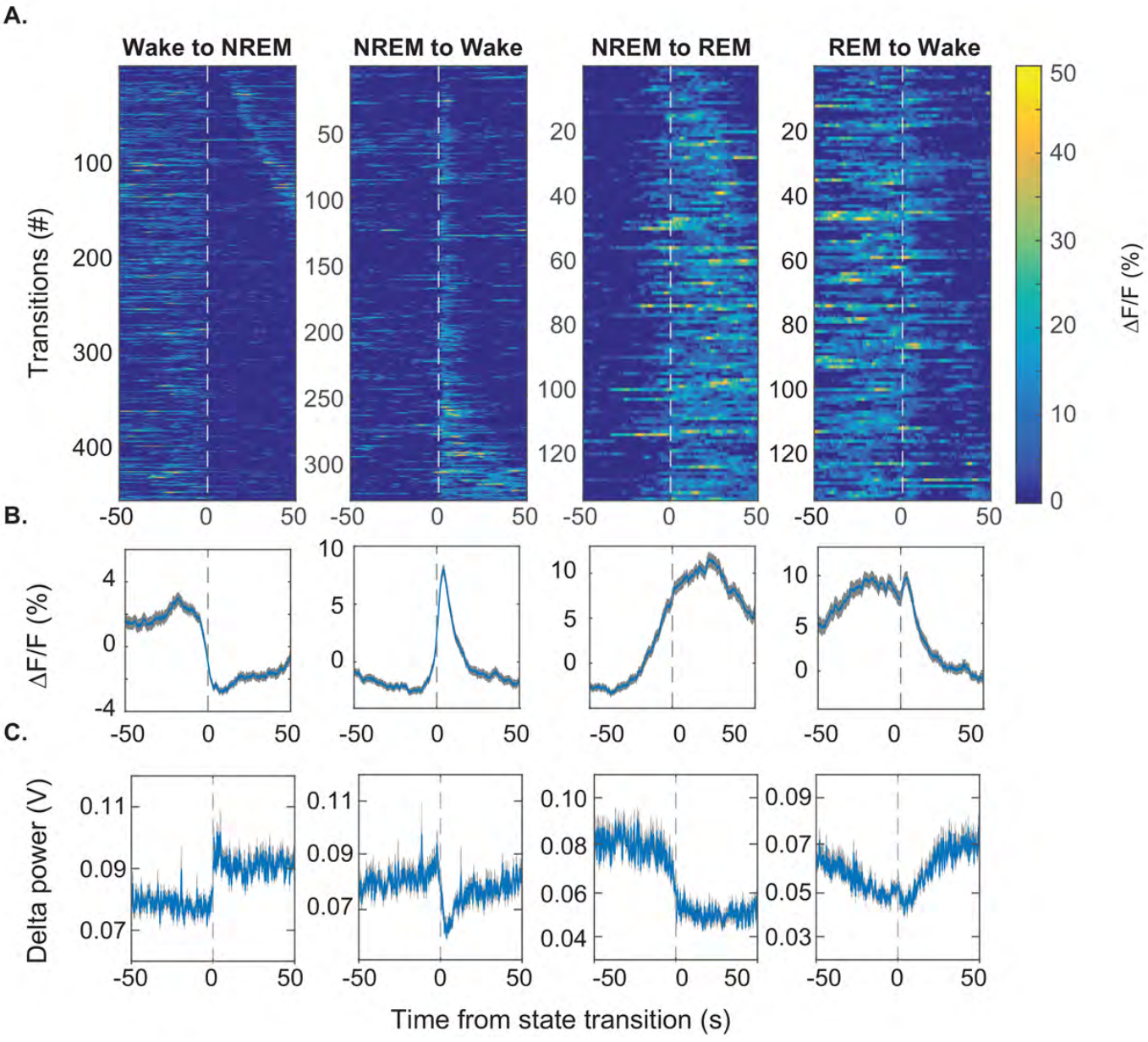

eNeuro Accepted Manuscript

Figure 3

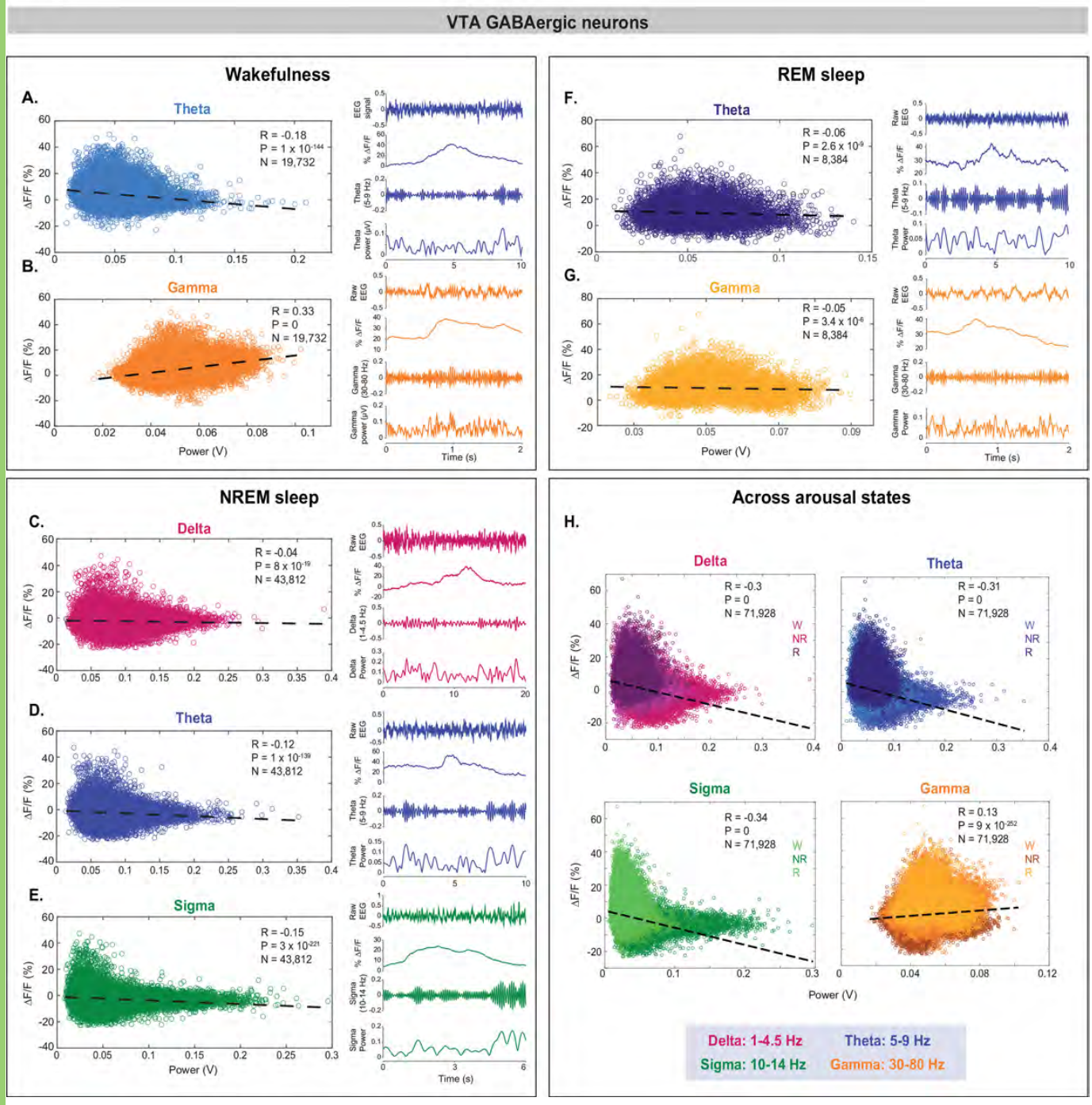

eNeuro Accepted Manuscript

Figure 4

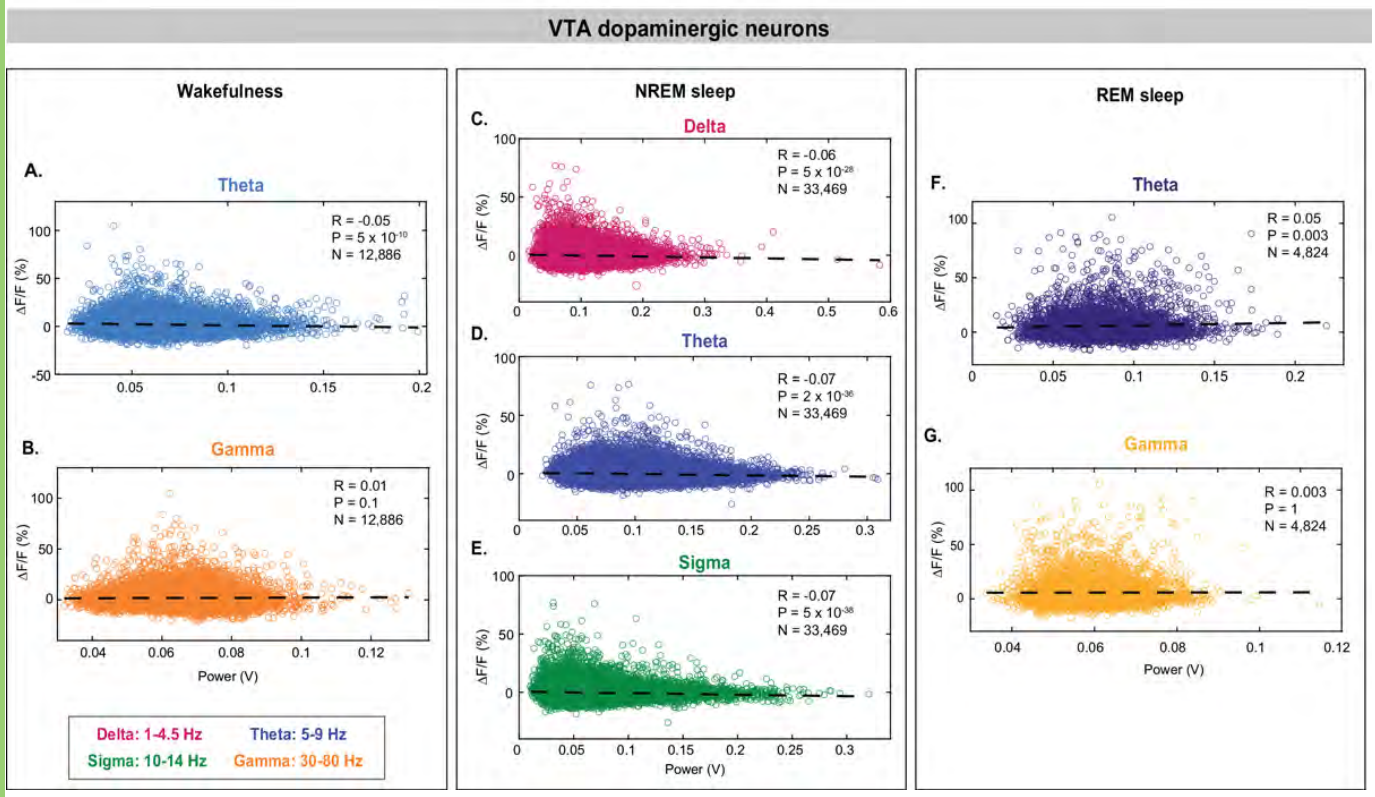

eNeuro Accepted Manuscript
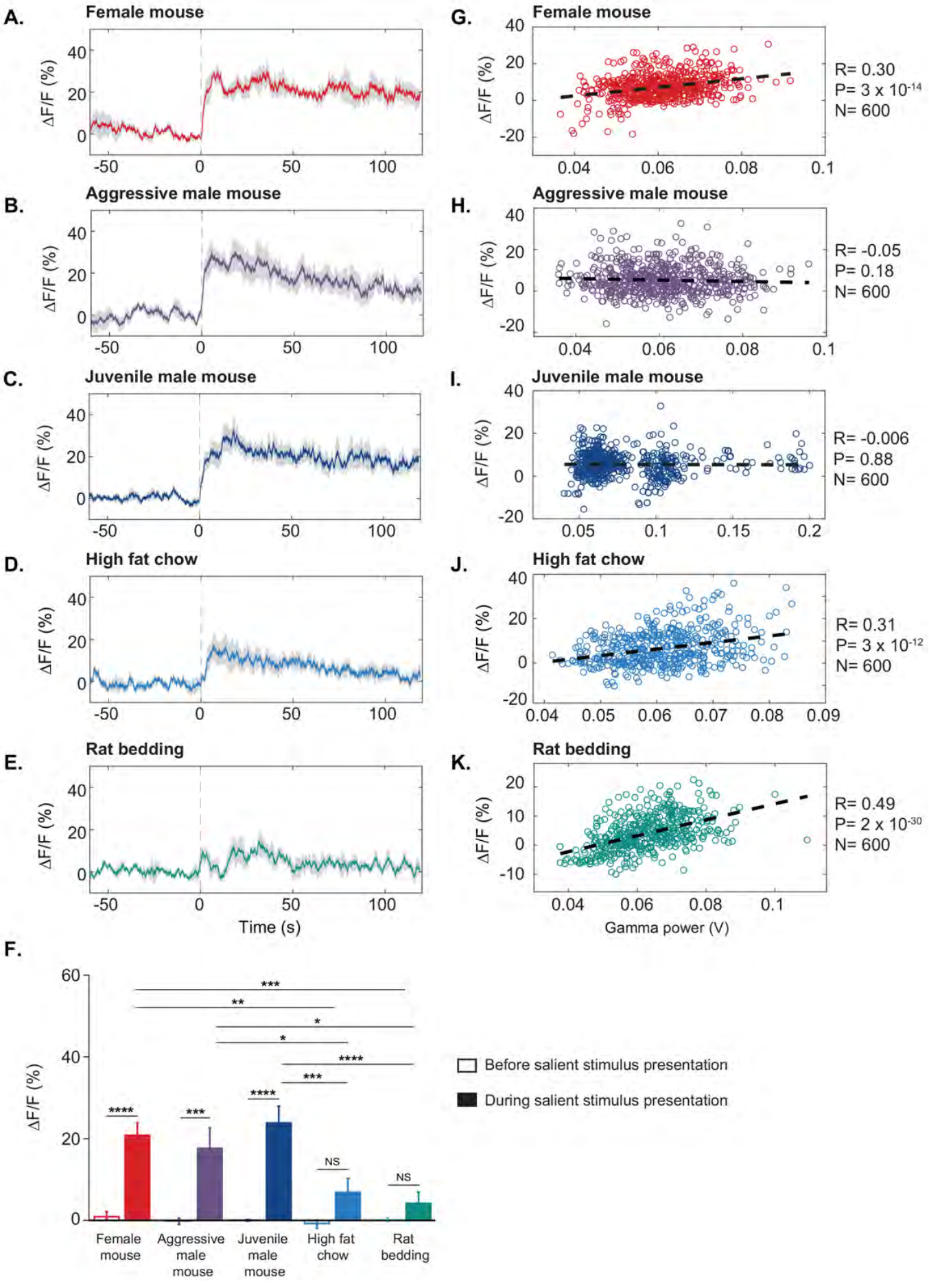
Figure 5